Supplemental Materials

Molecular Biology of the Cell

Stepanyants et al.

Supplemental figure legends

Figure S1. Biochemical and biophysical characterization of Drp1 B-insert mutants. (A) Domain architecture of Drp1 (human isoform 3) and a color-coded representation of the crystal structure of a self-assembly defective Drp1 mutant that also lacks the B-insert (Frohlich et al., 2013) showing the predicted position (dotted trace) of the deleted polypeptide region. The four mutations in the B-insert that constitute Drp1 4KA (Bustillo-Zabalbeitia et al., 2014) as well as the residues deleted in Drp1 ΔB (Frohlich et al., 2013) are indicated. (**B**) Kinetics and amplitude of the FRET-sensitized increase in Rh-DOPE emission intensity upon addition of BODIPY-FL-labeled Drp1 WT or mutants (0.1 μM protein) to liposomes (10 μM total lipid). The traces are normalized with respect to the differential BODIPY-FL labeling efficiencies observed for the mutants. The data reveal that Drp1 4KA and Drp1ΔB are both defective in stable membrane association. (**C**) Confocal fluorescence images of Rh-DOPE-labeled, 25 mol% native CL-containing GUVs incubated in the presence of BODIPY-FL-labeled Drp1 4KA or Drp1 ΔB. Merged images are shown. Notice the lack of membrane tubulation for either mutant and the presence of a significant amount of unbound protein in the surrounding bulk solution for Drp1 ΔB. Scale bar, 5 μm. (**D**) The in-solution basal and the lipid-stimulated GTPase activities of Drp1 4KA and Drp1 ΔB on 25 mol% CL-containing liposomes are plotted in relation to Drp1 WT as specific activity ± SD (n=3). The final protein and lipid concentrations were 0.5 μM and 150 μM, respectively. (**E**) Confocal images of 25 mol% native CL-containing GUVs labeled with both TopFluor-CL and Rh-DOPE upon addition of Drp1 4KA or Drp1 ΔB (0.5 μM protein final). **(F)** Intensity line profiles display the degree of TopFluor-CL aggregation in GUVs upon addition of either Drp1 4KA or Drp1 ΔB. The degree of membrane condensation is represented as intensity ratios of the TopFluor-CL-aggregated and –non-aggregated regions. A greater ratio indicates a higher degree of membrane condensation. Scale bar, 5 μm.

Figure S2. Calcium concentration- and DOPE-dependence of apparent lamellar-to-H_{II} membrane phase transition. (A) NBD emission intensity increase in NBD-DOPE-incorporated liposomes containing 25 mol% native CL in the presence of DOPC and DOPE (50 μM total lipid), upon addition of $CaCl_2$ to either 5 mM or 25 mM final. (**B**) NBD emission intensity increase in liposomes (50 μM total lipid) containing 25 mol% native CL in the absence or presence of DOPE (35 mol%), upon addition of $CaCl_2$ (25 mM final). (**C**) NBD emission intensity increase in liposomes (50 μM total lipid) containing 25 mol% native CL in the absence or presence of DOPE (35 mol%), upon addition of Drp1 WT (0.5 μM final).

Figure S3. Drp1 exclusively remodels native CL-containing GUVs in the presence of GTP. (A) Confocal fluorescence images of phase-separated TMCL-containing GUVs (left panel) displaying co-existing Rh-DOPE-labeled, fluid (red), and unlabeled, raft-like (dark), membrane regions after addition of BODIPY-FL-labeled Drp1 WT (0.5 μM protein final; middle panel) in the constant presence of GTP. No remodeling is observed. A merged image is shown to the right. Scale bar, 5 μm. (**B**) Representative confocal fluorescence images of the extent of membrane remodeling in Rh-DOPE-labeled, 25 mol% native CL-containing GUVs as a function of BODIPY-FL-labeled Drp1 WT concentration, in the absence or presence of GTP (1 mM final). Merged images are shown. % GUVs tubulated in the absence of GTP or constricted in the presence of GTP are indicated in the upper right hand corner of each image. Slender arrows in the "no nucleotide" panels point to Drp1-decorated membrane tubules, whereas in the "GTP" panels, they point to constricted "membrane buds". Block arrows in the "GTP" panels point to condensed membrane regions that may constitute sites of extensive lamellar-to-H_{II} CL phase transition. Scale bar, 5 μm.

Figure S4. Biochemical and biophysical characterization of Drp1 GTPase domain mutants. (A) Color-coded representation of the Drp1 crystal structure as in Figure S1A, but with the GTPase domain mutations highlighted and represented in space-fill. (**B**) GTPase activities of Drp1 GTPase domain mutants on 25 mol% CL-containing liposomes are plotted in relation to Drp1 WT as concentration of inorganic phosphate (P_i) released over time (n=3, ± SD). The final protein and lipid concentrations were 0.5 μM and 150 μM, respectively. (**C**) Representative confocal fluorescence images displaying differential remodeling of Rh-DOPE-labeled, 25 mol% CL-containing GUVs by BODIPY-FL-labeled-Drp1 GTPase domain mutants in the absence or presence of various nucleotides. Only merged images are shown. Slender, block and contour arrows point to membrane tubules, solution protein aggregates and membrane constrictions, respectively. Scale bar, 5 μm. (**D**) Velocity spin-sedimentation profiles for Drp1 GTPase domain mutants in the absence or presence of various nucleotides in solution plotted in comparison to Drp1 WT as '% Drp1 pelleted'. Values are averages of two independent experiments.

Figure S5. TMCL-containing liposomes resist GTP-dependent membrane constriction. (A) Representative negative-stain EM images of Drp1-decorated TMCL-containing liposomes before and after addition of GTP. **(B)** Effect of GDP addition on the morphology of Drp1-decorated, native CL-containing membrane tubules. A representative image is shown. Scale bar, 200 nm.

Figure S1

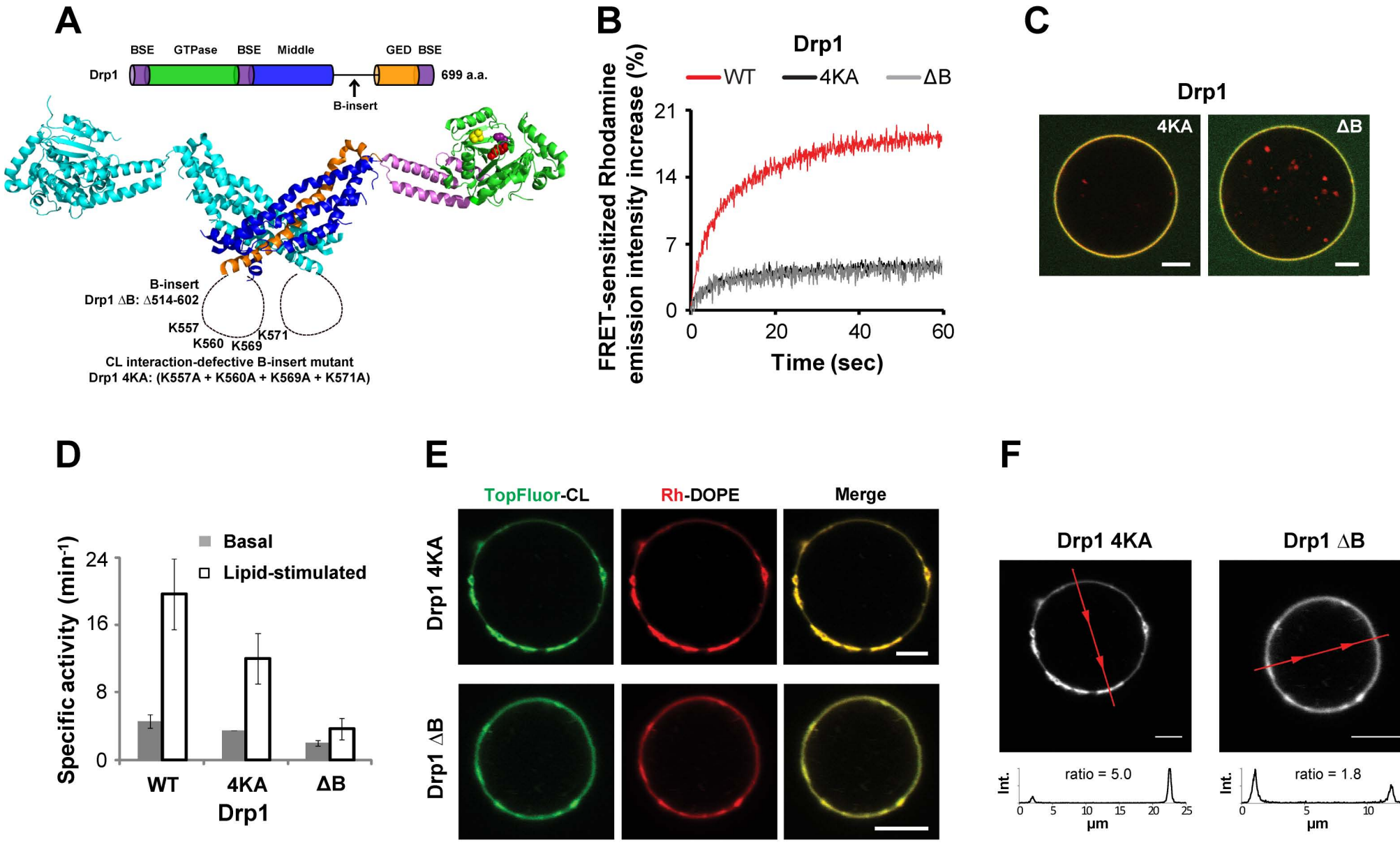
A
BSE GTPase BSE Middle GED BSE
Drp1
699 a.a.
B-insert
B-insert
Drp1 ΔB: Δ514-602
K557
K560 K569
K571
CL interaction-defective B-insert mutant
Drp1 4KA: (K557A + K560A + K569A + K571A)
B
Drp1
WT
4KA
ΔB
FRET-sensitized Rhodamine emission intensity increase (%)
21
14
7
0
0
20
40
60
Time (sec)
C
Drp1
4KA
ΔB
D
Basal
Lipid-stimulated
Specific activity (min-1)
24
16
8
0
WT
4KA
ΔB
Drp1
E
TopFluor-CL
Rh-DOPE
Merge
Drp1 4KA
Drp1 ΔB
F
Drp1 4KA
Drp1 ΔB
ratio = 5.0
ratio = 1.8
Int.
0
5
10
15
20
25
μm

Figure S2

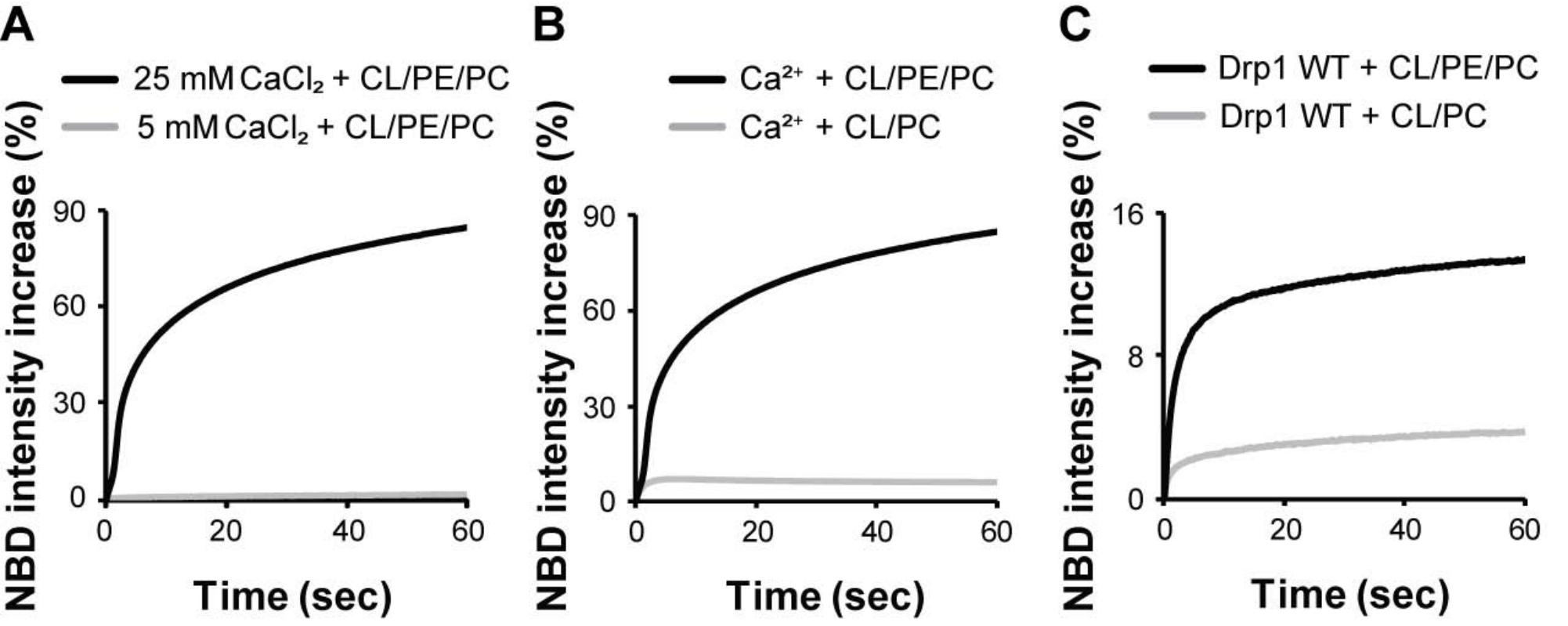
A
25 mM CaCl2 + CL/PE/PC
5 mM CaCl2 + CL/PE/PC
NBD intensity increase (%)
90
60
30
0
0
20
40
60
Time (sec)
B
Ca2+ + CL/PE/PC
Ca2+ + CL/PC
NBD intensity increase (%)
90
60
30
0
0
20
40
60
Time (sec)
C
Drp1 WT + CL/PE/PC
Drp1 WT + CL/PC
NBD intensity increase (%)
16
8
0
0
20
40
60
Time (sec)

Figure S3

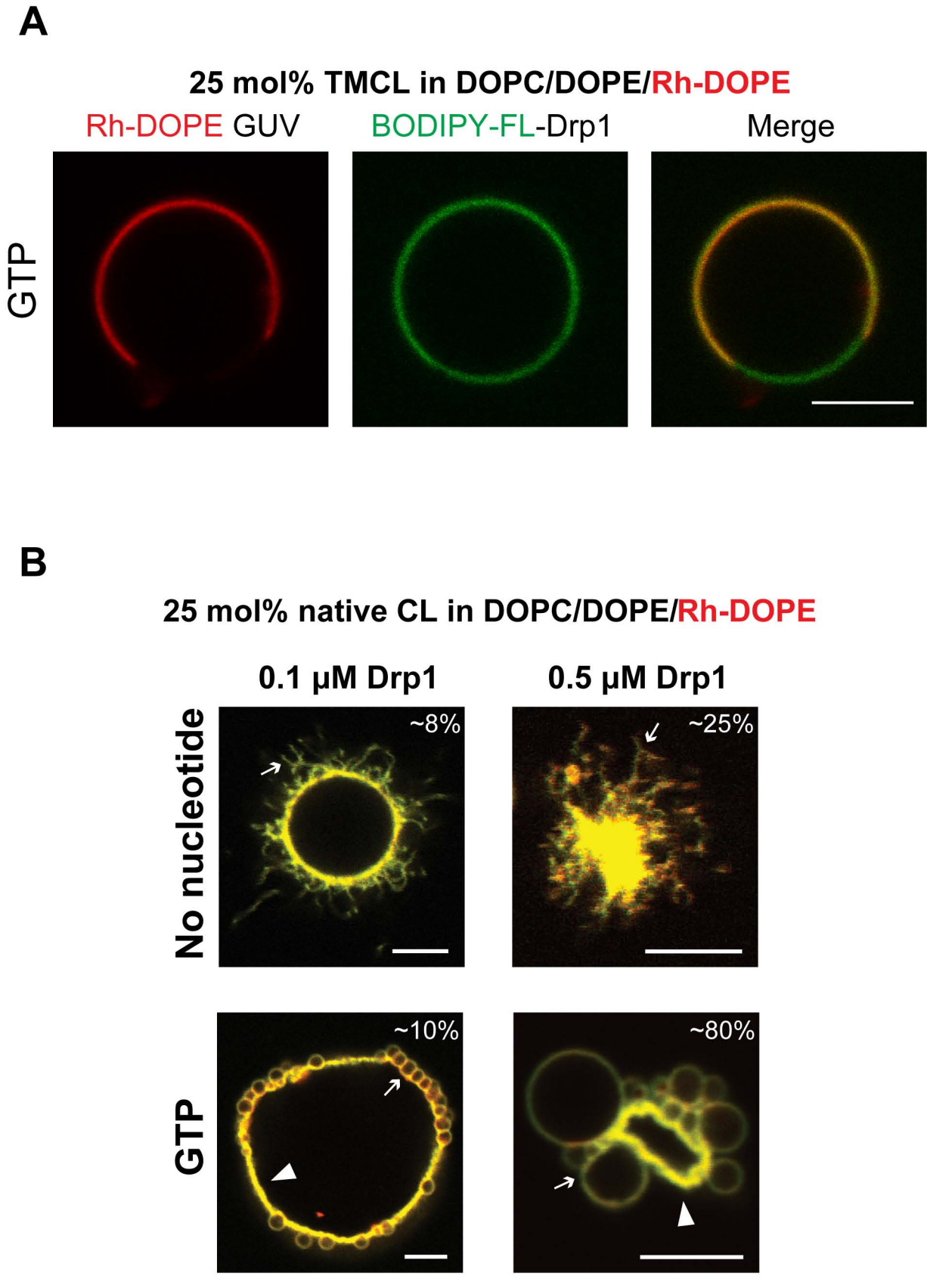
A
25 mol% TMCL in DOPC/DOPE/Rh-DOPE
Rh-DOPE GUV
BODIPY-FL-Drp1
Merge
GTP
B
25 mol% native CL in DOPC/DOPE/Rh-DOPE
0.1 μM Drp1
0.5 μM Drp1
No nucleotide
~8%
~25%
GTP
~10%
~80%

Figure S4

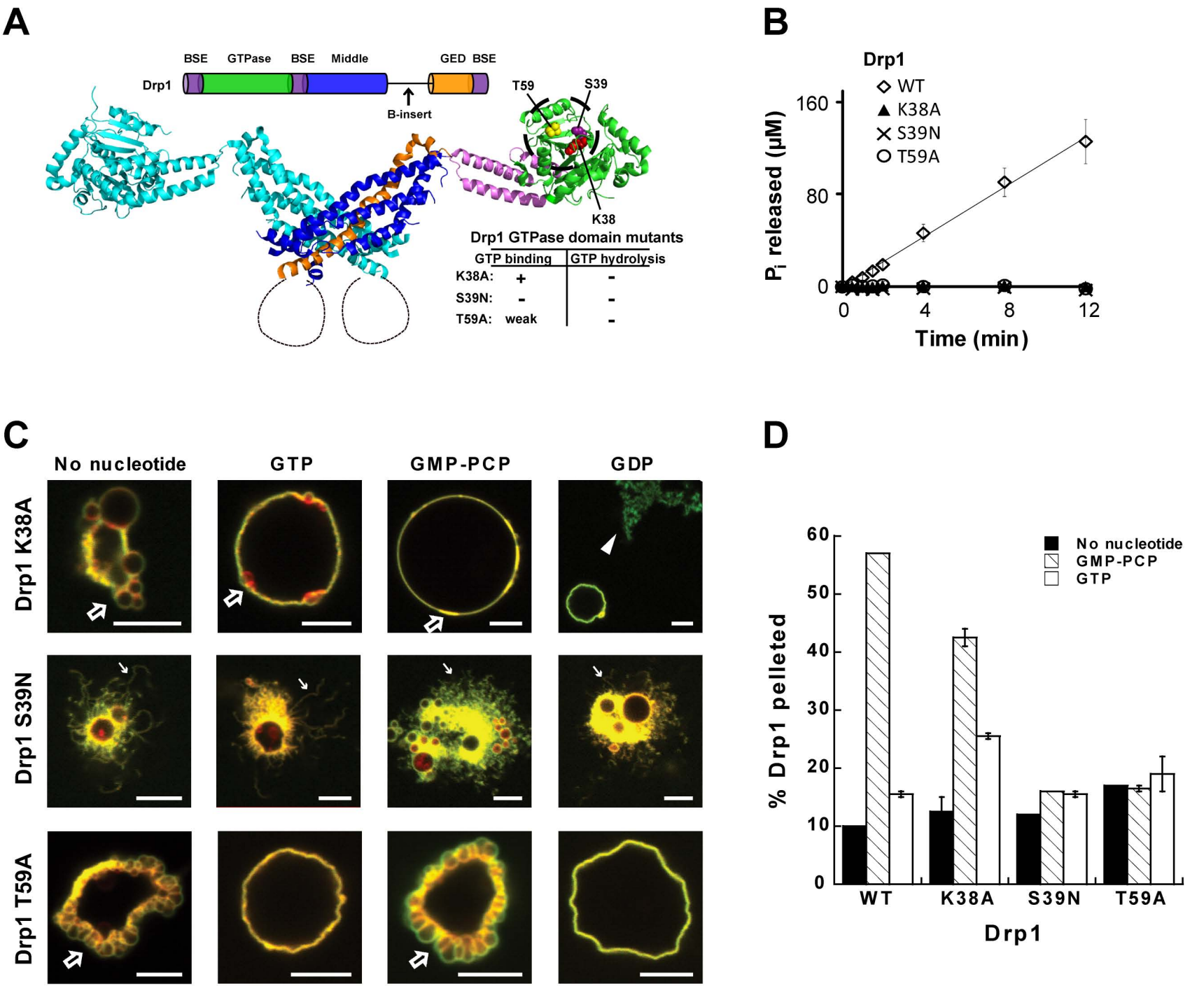
A
BSE GTPase BSE Middle GED BSE
Drp1
B-insert
T59
S39
K38
Drp1 GTPase domain mutants
GTP binding | GTP hydrolysis
K38A: + -
S39N: - -
T59A: weak -
B
Drp1
WT
K38A
S39N
T59A
P_i released (μM)
160
80
0
0
4
8
12
Time (min)
C
No nucleotide
GTP
GMP-PCP
GDP
Drp1 K38A
Drp1 S39N
Drp1 T59A
D
No nucleotide
GMP-PCP
GTP
% Drp1 pelleted
60
50
40
30
20
10
0
WT
K38A
S39N
T59A
Drp1

Figure S5

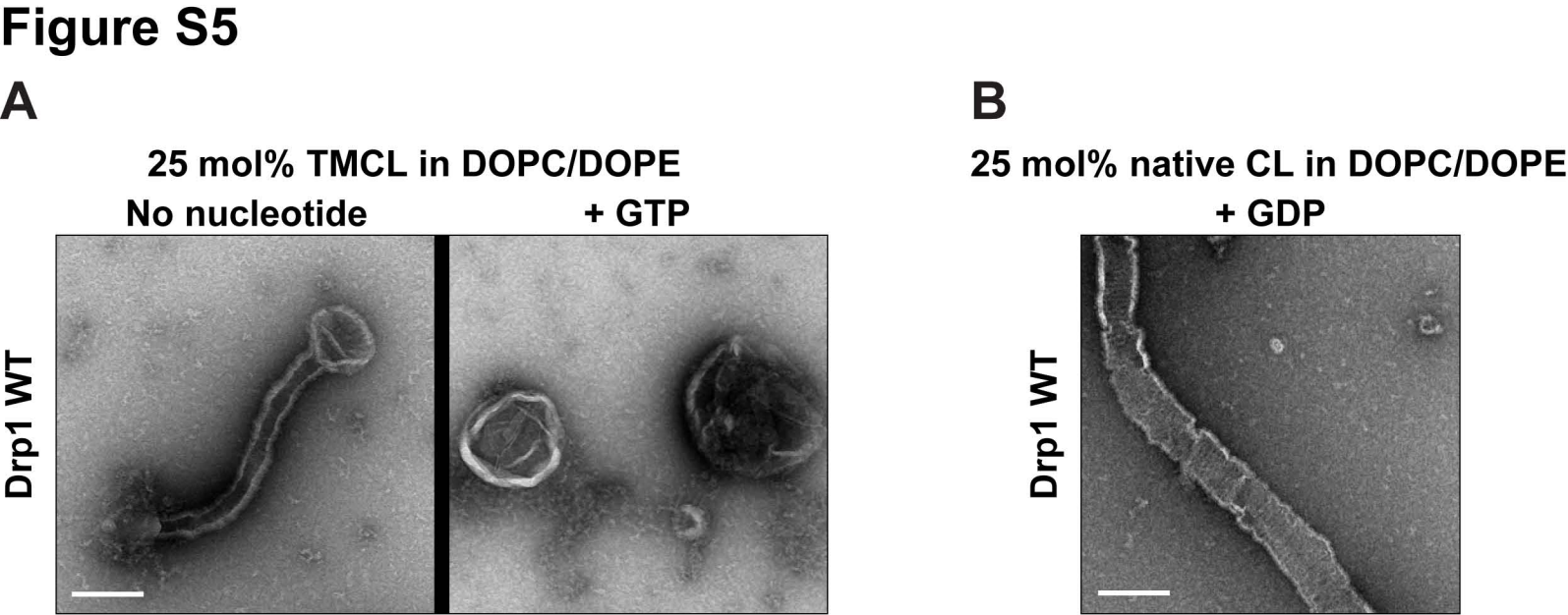
A
25 mol% TMCL in DOPC/DOPE
No nucleotide
+ GTP
Drp1 WT
B
25 mol% native CL in DOPC/DOPE
+ GDP
Drp1 WT